Separation Science and Technology
Publication details, including instructions for authors and subscription information:
http://www.informaworld.com/smpp/title~content=t713708471

Method for Online Process Monitoring for Use in Solvent Extraction and Actinide Separations

Jamie Warburton[a]; Nick Smith[a]; Ken Czerwinski[a]
[a] Department of Chemistry and Harry Reid Center for Environmental Studies, University of Nevada Las Vegas, Las Vegas, NV, USA

Online publication date: 30 August 2010

To cite this Article Warburton, Jamie , Smith, Nick and Czerwinski, Ken(2010) 'Method for Online Process Monitoring for Use in Solvent Extraction and Actinide Separations', Separation Science and Technology, 45: 12, 1763 — 1768
To link to this Article: DOI: 10.1080/01496395.2010.494085
URL: http://dx.doi.org/10.1080/01496395.2010.494085

Separation Science and Technology, 45: 1763–1768, 2010

ISSN: 0149-6395 print/1520-5754 online
DOI: 10.1080/01496395.2010.494085

Taylor & Francis
Taylor & Francis Group

Method for Online Process Monitoring for Use in Solvent Extraction and Actinide Separations

Jamie Warburton, Nick Smith, and Ken Czerwinski
Department of Chemistry and Harry Reid Center for Environmental Studies, University of Nevada Las Vegas, Las Vegas, NV, USA

UV-Visible spectroscopy can be utilized in an on-line fashion to directly measure the concentration and speciation of special nuclear materials, such as uranium and plutonium, thus allowing real-time process control and tracking for the solvent extraction processes. Attributing UV-Visible data to process conditions is complex due to uranyl nitrate speciation, thus efforts focus on characterizing the system encompassing 0.01–1.26 M U and 0.01-8 M HNO_3. Results suggest dominant speciation changes from low (0.01 M) to high (>6 M) HNO_3, and peak shifts in the high (>1 M) uranyl system imply an ingrowth of species not present at lower uranyl concentrations.

Keywords online monitoring; reprocessing; uranyl nitrate speciation; UREX; UV-Visible spectroscopy

INTRODUCTION

Spectroscopic investigations allow direct characterization of the physiochemical state of a metal ion in solution and provide thermodynamic data on its prevailing species (1,2). The UV-Visible absorbance occurs at specified wavelengths due to the bond energetics of the analyte under investigation. When photons of a characteristic absorbance wavelength are passed through the sample, the absorbing species acquires an electronically excited state. Based on electronic configurations, metals can undergo a variety of transitions between orbitals. The transitions of the 5f orbital electrons are of interest in this work, since the molecule being excited is the uranyl ion (UO_2^{2+}), and the 5f shell contains the highest occupied orbital. The molecular orbital diagram of the uranyl ion demonstrates orbital mixing of the 5f (U) and 2p (O) and shows the highest occupied orbitals (σ_g, σ_u, π_g, π_u), along with the lowest unoccupied orbitals (σ_g, σ_g) which are important in excitation and bonding and have only f orbital contributions (3).

Received 19 October 2009; accepted 17 March 2010.
Address correspondence to Jamie Warburton, Department of Chemistry and Harry Reid Center for Environmental Studies, University of Nevada Las Vegas, 4505 Maryland Parkway, Las Vegas, NV 89154, USA. E-mail: warburt5@unlv.nevada.edu

The uranyl ion has characteristic absorption spectra containing three fingerlike peaks at 403, 414, and 426 nm (Fig. 1). The uranyl absorption spectra change shape and shift absorbance maxima with changes in speciation, since the spectrophotometer detects variations in the uranium electron configuration and transition energies. Changes in speciation can occur due to variations in ligand and metal concentration with previous work showing that as nitric acid concentration increases from 2 to 6 M the characteristic uranyl peaks broaden and merge into one large peak (4).

In general, UV-Visible spectroscopy is a reliable method for uranium concentration determination. However, this work exploits a main caveat to this generalization, which is that uranyl measurement by UV-Visible spectroscopy in nitrate matrices is complex due to nitrate concentration altering uranyl speciation, and therefore its absorption spectrum (4). The uranyl nitrate complex usually exists as the dinitrate $UO_2(NO_3)_2$; however, it has been reported that the uranyl trinitrato complex was prepared at upwards of 16 M HNO_3 and found to be fairly stable in the absence of water (5). Additionally, the tetranitrato complex, $[UO_2(NO_3)_4]^{2-}$ has been demonstrated in the absence of water and at upwards of 20 M HNO_3. The molar extinction coefficient of the tetranitrato salt is much higher than that of the trinitrato salt and is reported to reach upwards of 57 $M^{-1}cm^{-1}$, as compared to 8–10 $M^{-1}cm^{-1}$ for the latter (5).

In considering the application of spectroscopy in a separations scheme, typical output streams from the PUREX/UREX fuel recycling process contain up to 300 g/L uranium ($\leq$1.26 M), in addition to approximately 0.1–6 M nitric acid and corresponding ranges of nitrate. Additionally, centrifugal contactors have been found to be reliable, relatively inexpensive to build, operate, and maintain, and therefore have been considered for use in a reprocessing plant. Due to the compact contactor stages, the overall liquid holdup is low, the systems can undergo fast startup and shutdown, and high mass transfer efficiency can be achieved (6). The contactor interstage

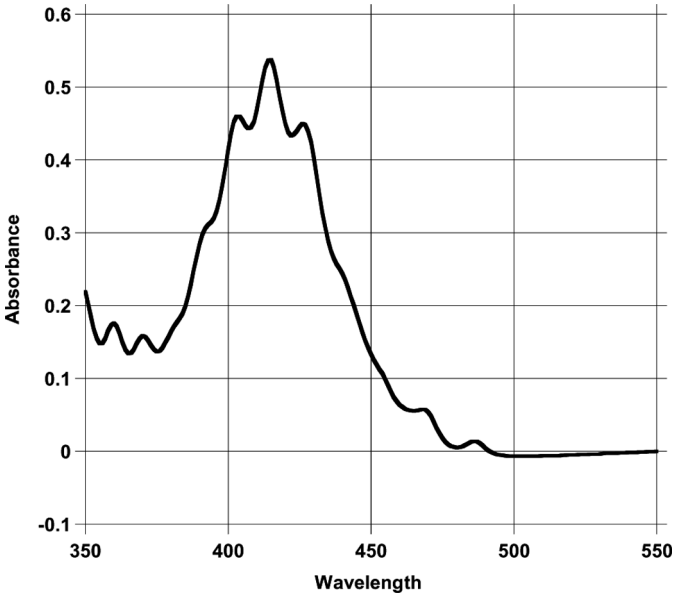

FIG. 1. UV-Visible absorbance of 0.63 M U at 0.01 M HNO_3.

lines are external to the contactor body so that both the aqueous and organic phases are accessible as they enter and leave each stage, making stream interrogation physically straightforward. Thus, the process monitoring system described in this work is applied to a contactor setup for a demonstration of the technology and methodology.

In the visible uranium spectrum, the 426 nm absorption line possesses the greatest sensitivity to nitrate (with concentrations altered via introduction of nitric acid) conditions, whereas the 359 nm line exhibits a sensitivity which is only one-third of this value. Overall, the absorption at all wavelengths increases with nitric acid concentration – the 403, 426, and 416 nm uranium triplet becomes less defined, as the 426 nm line broadens into a shoulder. In the literature, the slopes of the curves obtained with varying nitrate were found to be identical to those obtained with varying nitric acid, with uranyl absorbance demonstrating a linear relationship with nitrate throughout the uranium concentration range (4).

Theoretical proliferant diversions in separations would be accomplished via deliberate modification of the flowsheet chemistry; therefore, by confirming proper operational performance and verifying process integrity throughout the PUREX/UREX scheme, these diversions can be identified. Online, real time, multiparametric monitoring of the radiochemical streams in a reprocessing flowsheet can provide rapid detection of unwanted deviations from normal operation conditions. In order to effectively monitor a reprocessing scheme, the key signatures, namely concentration and speciation of the main components, of the separations under normal conditions must be identified as to have a reference case. Additionally, the stream pH, flow rate, and temperature can be monitored and compared with chemical libraries of spectroscopic, chemical and physiochemical properties (7).

EXPERIMENTAL

In a flowing system, there are two methods for the UV-Visible spectroscopy of the moving solutions—a fiber optic dip probe can be inserted into the stream or the stream can be diverted to a cuvette flow-cell placed in a spectrophotometer. Studies of both systems are presented here.

In preliminary studies, an Ocean Optics fiber optic dip probe was inserted into a Swagelok tee with a diaphram pump providing solution flow, and a system containing 0.0113–0.566 M [UO_2^{2+}] was investigated with the Ocean Optics USB2000+UV-Visible spectrometer system using a 2 mm pathlength tip. Next, the fiber optic dip probe was mounted in a Swagelok tee design in the product stream of bank of 20, 2-cm contactors at Argonne National Laboratory (ANL) where a uranium only UREX demonstration was performed.

As an alternative to the fiber optic dip probe technique, quartz Hellma flow-through cuvettes with pathlengths of 0.1, 0.5, and 1.0 cm were coupled with a peristaltic pump (flowrate $\leq$2.5 mL/min) and a Cary 6100 Spectrophotometer. These cuvettes are very similar to standard cuvettes for UV-Visible spectrophotometric measurements, however, the concept is that a slipstream of the solution of interest can be directed into a benchtop spectrophotometer as to provide higher resolution data. Samples of 0.01, 0.126, 0.262, 0.63, 1 and 1.26 M U at 0.01, 0.1, 0.5, 1, 3, and 6 M HNO_3 were prepared via dilution of a single stock uranyl nitrate solution. The $UO_2(NO_3)_2$ solution was prepared gravimetrically by dissolving 141.11 g of $UO_2(NO_3)_2 \cdot 6H_2O$ in 200 mL of DI H_2O to make a 1.4 M stock from which samples were prepared by volumetric dilution with concentrated HNO_3 and DI H_2O. Prepared samples were analyzed by ICP-AES using a NIST traceable standard at 9962 ± 37 ppm for calibration with $R^2 = 0.9997$ and all samples were found to have less than 1.5% error across triplicates. The samples were then pumped through the Hellma cuvettes using the peristaltic pump, and UV-Visible spectra were obtained in triplicate at a flowrate of approximately 2 mL/minute with the Cary 6100 in double beam mode with a quartz cuvette of DI H_2O as a background. Reported spectra are averaged and background subtracted.

Next, samples were prepared at 2, 4, 5, 7, 8 M HNO_3 with 0.01, 0.126, 0.262, 0.63, and 1 M UO_2^{2+} via volumetric dilution (with concentrated HNO_3 and DI H_2O) of a single stock uranyl nitrate solution characterized as 1.9 M $UO_2(NO_3)_2$ in 0.9 M HNO_3 by ICP-AES and titration. Again, all samples were analyzed by ICP-AES using a NIST traceable standard at 9962 ± 37 ppm for calibration

with $R^2 = 0.9998$ and less than 2.8% error was found across triplicates. These samples were titrated along with samples previously prepared using a potassium oxalate complexation method and a standardized 0.1 M NaOH solution. The average disagreement between the expected and titrated acid concentrations for all samples was found to be 7.77%. As nitric acid was the only acid used in these experiments, acidities are directly correlated to nitric acid and therefore nitrate concentrations. Again, the samples were then pumped through the Hellma cuvettes using the same experimental setup and conditions as used previously, with reported spectra averaged and background subtracted.

DISCUSSION AND RESULTS

As seen in Fig. 2, the Ocean Optics setup can easily and distinctly resolve 0.04 M differences in UO_2^{2+} concentration at levels as low as 0.01 M UO_2^{2+}, and can provide some spectral information at concentrations upwards of 0.5 M UO_2^{2+}, however, the characteristic uranyl shape is lost and peaks cannot be resolved.

To continue studies with the fiber optic probe UV-Visible spectroscopy system, solutions with varying concentrations of Nd were used in order to determine the time response of the probe in solution. Results indicate instantaneous response from the probe when presented with 0.02 M differences in concentration of $Nd(NO_3)_3$ (Fig. 3).

A similar time response experiment was conducted with the fiber optic probe setup; however, varying concentrations of uranyl nitrate were used, and the resolution (minimum distinguishable concentration difference) was found to be 0.002 M $UO_2(NO_3)_2$ (Fig. 4).

After scoping studies with the Swagelok tee and single-pump system, the fiber optic probe was mounted in the same Swagelok tee design in the product stream of bank of 20, 2-cm contactors at ANL for a uranium only

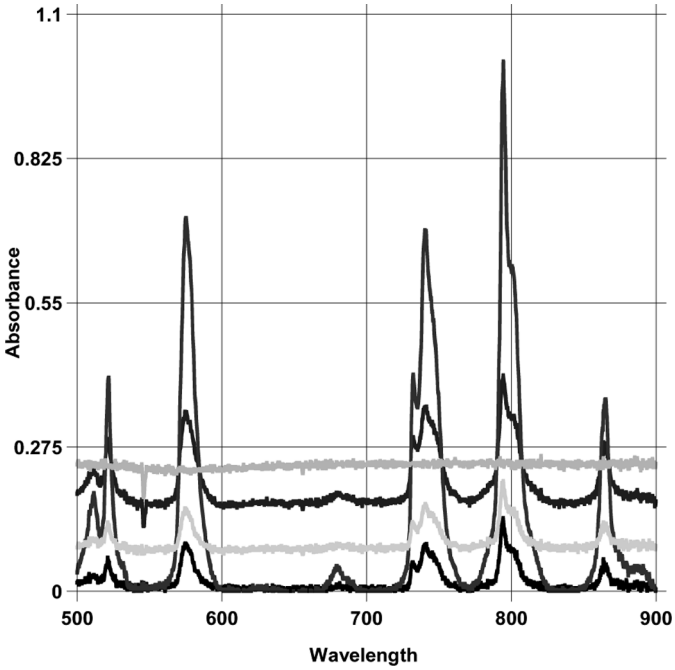

FIG. 3. Time response study with fiber optic dip probe in Nd solutions.

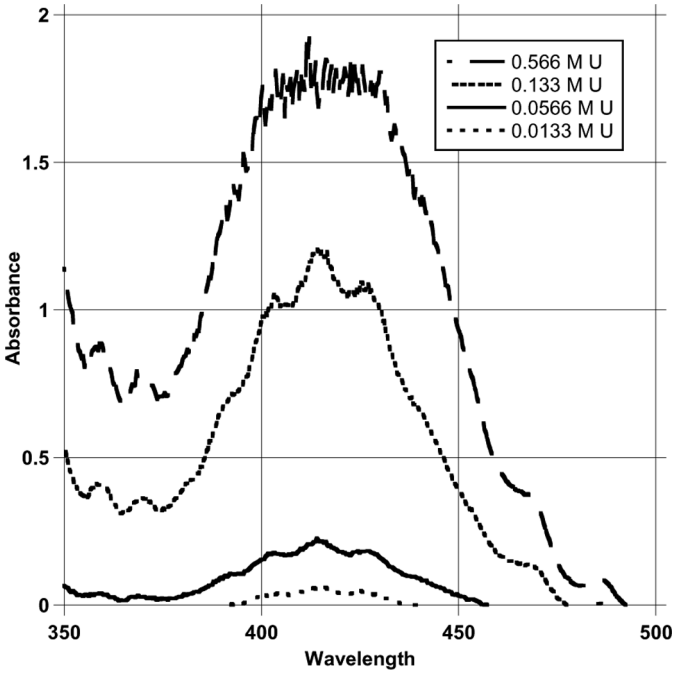

FIG. 2. Fiber optic dip probe range study with UO_2^{2+}.

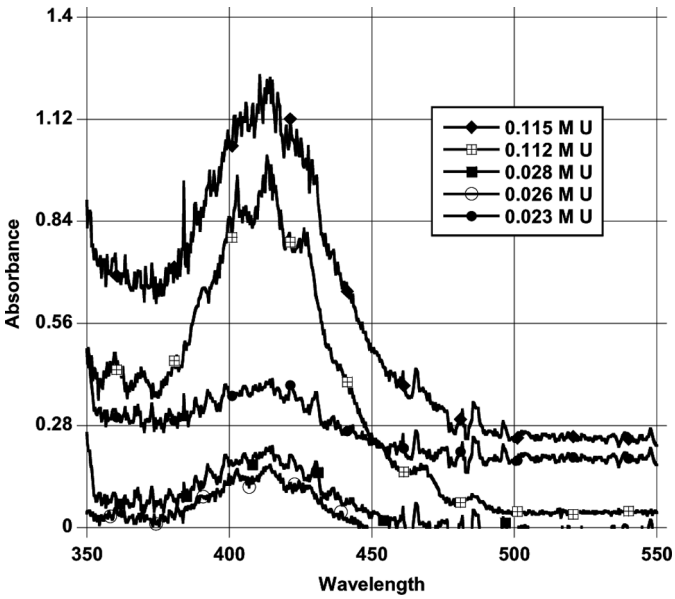

FIG. 4. Resolution studies with the fiber optic dip probe in Swagelok flow cell.

UREX demonstration. The introduction and growth of the UO_2^{2+} spectra as UO_2^{2+} enters the product stream exiting the last strip stage after approximately 30 minutes is shown in Fig. 5. The fiber optic probe behaved as expected in this demonstration, and the relationship between the solution flow rates and UV-Visible spectra was brought to attention. While there was no effect of the flow rate on spectra in previous experiments with a single solution flow, the countercurrent nature of the contactors combined with the use of multiple solution inlets complicates the relationship. Specifically, changes in the strip flow rate were found to be inversely proportional to the concentration changes in the product as seen by the UV-Visible spectrometer. In general, the flowrate of the solution under fiber optic dip probe investigation should be explicitly related to the other flowsheet flowrates, and this determined relationship can be used to explain UV-Visible absorbance value changes due to flowrate variance.

Next, in contrast to the fiber optic dip probe setup in which the measuring instrument is brought to the solution of interest, the flow-through cuvettes were used along with the standard benchtop spectrophotometer to investigate solutions from 0.01–1.26 M U and 0.01–8 M HNO_3. Previous to this work, it was assumed that in acidic solutions from pH ~ 0.1 to pH ~ 2, the uranyl ion UO_2^{2+} (U(VI)) would be exclusively formed (9), however, UV-Visible spectroscopy results suggest that instead, uranyl exists as a mixed species, likely the free ion, mono-, and di-nitrato.

The calculation of the uranyl nitrato complexes is not well defined as only the first complexation constant has been reported and reviewed (10). Some data is available for the second uranyl nitrate complexation constant, but nothing definitive or reviewed, and the tri- and tetranitrato complexes have been found in exotic nitric acid media, but their existence in lower concentrations has not been proven.

Although the calculation of uranyl nitrate speciation is unknown and complex, the speciation changes can be investigated spectroscopically. In Fig. 6, some semblance of the characteristic uranyl spectra can be seen throughout the range of nitric acid concentrations (0.01–8 M), however at 1.26 M UO_2^{2+} (Fig. 7), the characteristic uranyl spectra begins to lose shape immediately as nitric acid concentration increases, indicating prominent changes in speciation. The combination of 1.26 M UO_2^{2+} and 5 M HNO_3 concentration demonstrates the most defined spectral contrast when compared with the 0.126 M at 0.01 M HNO_3. Furthermore, changes in peak ratios are evident even in a cursory comparison of these figures, with the 403 peak being larger than the 426 peak in the low acid ($\leq$1 M HNO_3) spectra in Fig. 6, whereas the opposite is true of the same peak comparison in Fig. 7. A brief calculation of the unit-less peak ratio from Fig. 6 yields approximately 1.125 for the 0.01 M HNO_3 data, whereas the same calculation from Fig. 7 yields 0.913. The spectral changes are so great, in addition to free uranyl, mono-, di-, perhaps even tri- nitrate speciation changes, uranyl-uranyl coordination may contribute (11). It should be noted that stock uranium samples prevented the simple formation of 1.26 M UO_2^{2+} at upwards of 5 M HNO_3.

The overall spectral shape and peak definition are of primary concern in the comparison across nitric acid concentrations, not absolute absorbtivity values as there

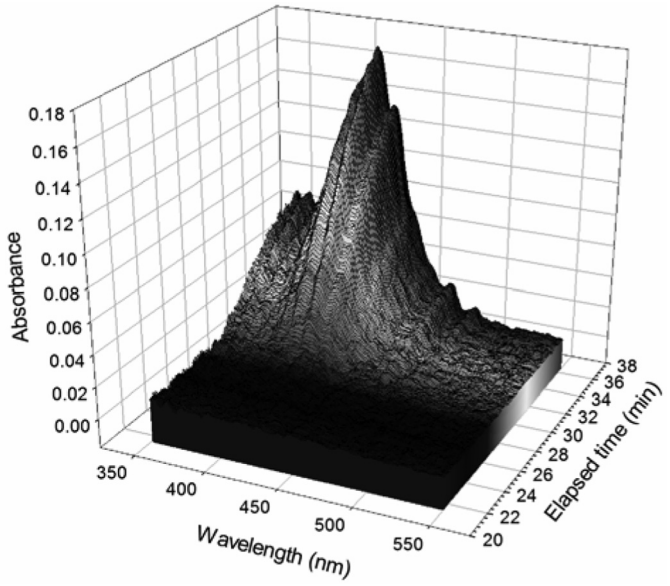

FIG. 5. UO_2^{2+} growth in UREX product stream (8).

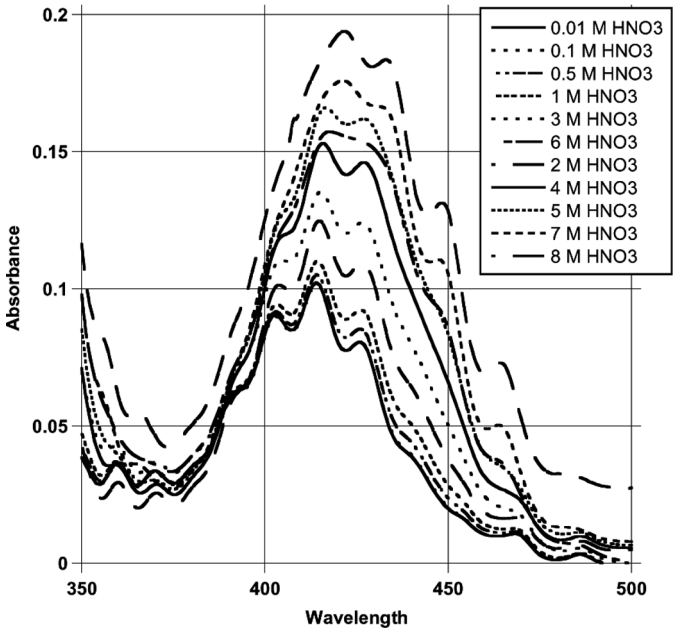

FIG. 6. UV-visible absorbance of 0.126 ± 0.02 M U at varied HNO_3.

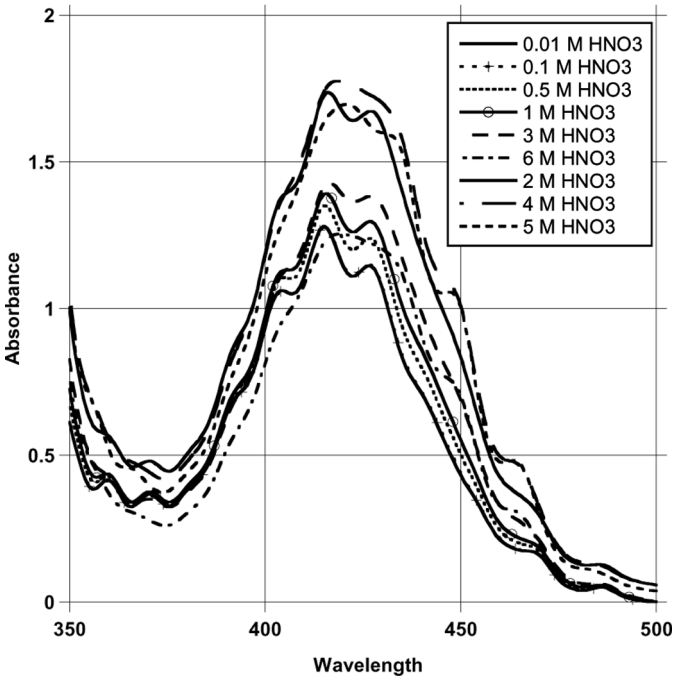

FIG. 7. UV-visible absorbance of 1.26 ± 0.10 M U at varied HNO_3.

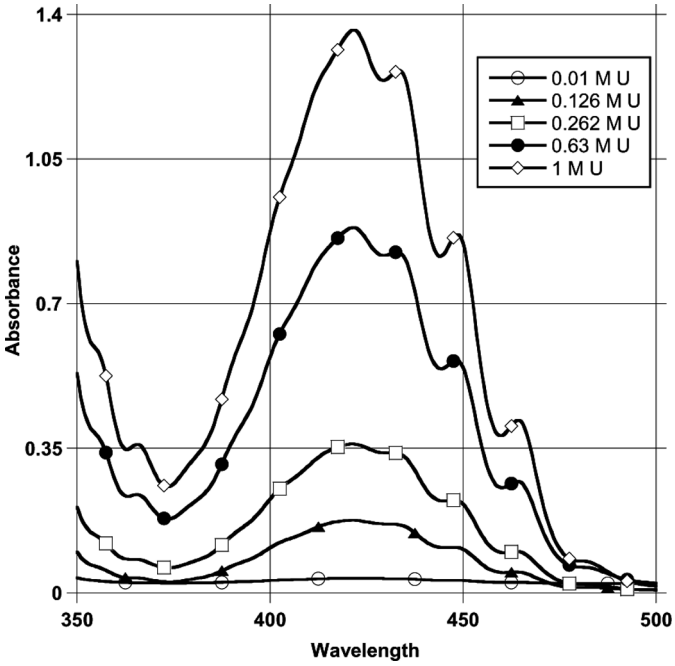

FIG. 9. UV-visible absorbance of varied U at 7 M HNO_3.

is a slight variance in uranyl concentration introduced in sample preparation. Figure 8 demonstrates the consistent characteristic uranyl spectra found at 0.01 M HNO_3 across all uranyl concentrations studied. In sharp contrast, Fig. 9 shows the complete lack of peak definition in the 380–410 nm range and the formation of defined peaks in the previously smooth 440–470 nm region for all uranyl concentration values.

Figure 10 describes the uranyl spectra at 3 M HNO_3 in mid-transformation from the characteristic shape observed

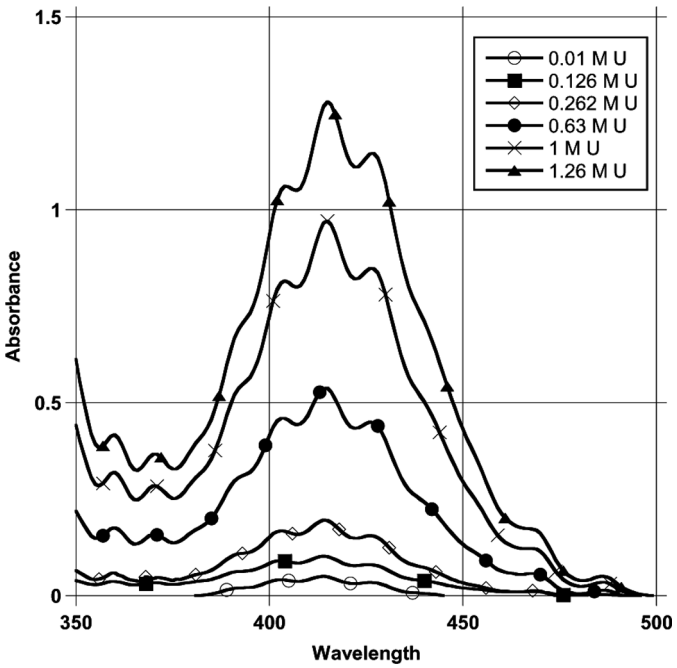

FIG. 8. UV-visible absorbance of varied U at 0.01 M HNO_3.

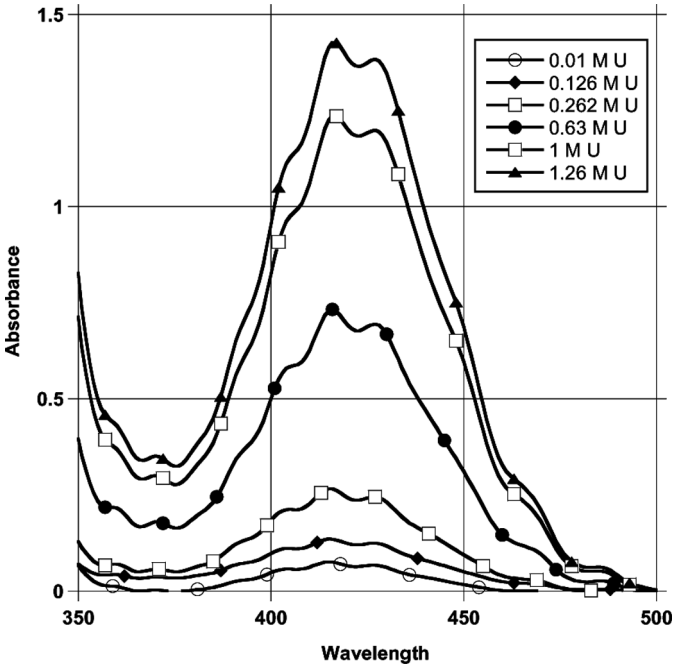

FIG. 10. UV-visible absorbance of varied U at 3 M HNO_3.

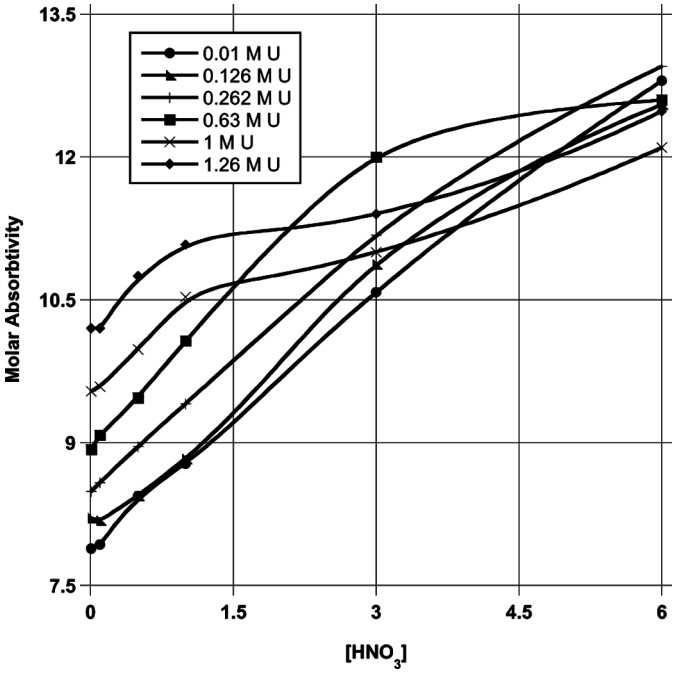

FIG. 11. Molar absorbtivities at 414 nm for uranyl in varied nitric acid.

at 0.01 M HNO_3 to the shifted, unresolved profile from the 7 M HNO_3 condition, with shape atypical of a uranium system.

A calculation of molar absorbtivities from UV-Visible absorbance values and known uranyl concentrations shows the dependence of the molar absorbtivity on nitric acid (and therefore nitrate) concentration. The trends seen in Fig. 11 are present at the 403 and 426 nm peaks as well, indicating that changes in nitrate influence all uranyl nitrato species formation in a similar fashion.

CONCLUSIONS

UV-Visible spectroscopy can be used effectively to discriminate changes in uranyl and nitric acid concentrations in the 0.01–1.26 M uranium and 0.01–8 M nitric acid system. Alterations of the characteristic uranyl UV-Visible spectral shape at high nitric acid suggest significant speciation changes, and peak shifts in the high uranyl system similarly imply an ingrowth of uranyl nitrate species not present at lower uranyl concentrations. The presence of the differing uranyl nitrate species is expected to substantially affect the UV-Visible absorption spectra, therefore by coupling with additional spectroscopic studies, UV-Visible spectral variations can be attributed directly to specific speciation changes. Additionally, uranyl-uranyl coordination may be the basis of the UV-Visible spectral shifts seen at high uranium concentrations. By defining uranyl and nitrate parameters for the various uranyl nitrate species, a continuous model for the UV-Visible spectra can be developed and used in a process monitoring application. An upcoming benchmark for this work is a demonstration of the UV-Visible spectroscopy process monitoring concept in centrifugal contactors under solvent extraction conditions. On the whole, the continuation of these efforts will enable an online materials accountability system as well as provide an attribution methodology for identifying diversion scenarios.

ACKNOWLEDGEMENTS

This work was performed under the Nuclear Forensics Graduate Fellowship Program which is sponsored by the U.S. Department of Homeland Security's Domestic Nuclear Detection Office and the U.S. Department of Defense's Domestic Threat Reduction Agency. Additional funding was provided by DOE contract No. DE-FG07-08ID14927. The authors thank Tom O'Dou and Trevor Low for their help and dedication in laboratory radiation safety.

REFERENCES

1. Meinrath, G.; Klenze, R.; Kim, J.I. (1996) Direct spectroscopic speciation of uranium(VI) in carbonate solutions. *Radiochimica Acta*, 74: 81–86.
2. Meinrath, G. (1997) Uranium(VI) speciation by spectroscopy. *Journal of Radioanalytical and Nuclear Chemistry*, 224 (1–2): 119–126.
3. Grenthe, I.; Drozdzynski, J.; Fujino, T.; Buck, E.C.; Albrecht-Schmitt, T.E.; Wolf, S.F. (2006) Uranium. In: *The Chemistry of the Actinide and Transactinide Elements*, Morss, L.R., Edelstein, N.M., Fuger, J., Katz, J.J., eds.; Springer: The Netherlands, Vol. 3, 577.
4. Bostick, D.T. (1978) *The Simultaneous Analysis of Uranium and Nitrate*; Oak Ridge National Laboratory Analytical Chemistry Division: Oak Ridge.
5. Ryan, J.L. (1961) Anion exchange and non-aqueous studies of the anionic nitrato complexes of the hexavalent actinides. *The Journal of Physical Chemistry*, 65 (7): 1099–1107.
6. Leonard, R.A.; Chamberlain, D.B.; Conner, C. (1997) Centrifugal contactors for laboratory-scale solvent extraction tests. *Separation Science and Technology*, 32 (1): 193–210.
7. Bryan, S.; Levitskaia, T. (2007) *Monitoring of UREX Radiochemical Processes for Enhanced Safeguards in Reprocessing Plant*; Pacific Northwest National Laboratory: Battelle.
8. Krebs, J.F. Argonne National Laboratory, Argonne, IL. Personal communication: Figures for Warburton, September 2008.
9. Ahrland, S. (1949) On the complex chemistry of the uranyl ion, Part I. The hydrolysis of the six-valent uranium in aqueous solutions. *Acta Chemica Scandinavica*, 3: 374–400.
10. Ingmar Grenthe, H.W. (2004) Chemical thermodynamics of uranium. In: *Chemical Thermodynamics*, Forest, H.W.a.I., ed.; Nuclear Energy Agency, p. 267–274.
11. Barnes, C.E.; Shin, Y.; Saengkerdsub, S.; Dai, S. (2000) EXAFS study of uranyl nitrate dimer at high and low temperature. *Inorganic Chemistry*, 39 (4): 862–864.